

# Mapping of the anomalous magnetotransport regime in the $\alpha$ -(BEDT-TTF)<sub>2</sub>MHg(SCN)<sub>4</sub> ( $M = \text{K, Tl}$ ) organic conductors

M. M. Honold

*Department of Physics, University of Oxford, The Clarendon Laboratory, Parks Road, Oxford OX1 3PU, United Kingdom*

N. Harrison

*National High Magnetic Field Laboratory, LANL, MS-E536, Los Alamos, New Mexico 87545*

M. V. Kartsovnik

*Walther-Meissner-Institut, Walther-Meissner-Strasse 8, D-85748 Garching, Germany*

H. Yaguchi\* and J. Singleton

*Department of Physics, University of Oxford, The Clarendon Laboratory, Parks Road, Oxford OX1 3PU, United Kingdom*

C. H. Mielke

*National High Magnetic Field Laboratory, LANL, MS-E536, Los Alamos, New Mexico 87545*

N. D. Kushch

*Institute of Chemical Physics Research, Russian Academy of Sciences, Chernogolovka, 142432, Russian Federation*

M. Kurmoo† and P. Day

*The Royal Institution, 21 Albemarle Street, London W1X 4BS, United Kingdom*

(Received 22 February 2000)

We present a comprehensive set of pulsed-magnetic-field measurements of the quasi-two-dimensional organic conductors  $\alpha$ -(BEDT-TTF)<sub>2</sub>MHg(SCN)<sub>4</sub> ( $M = \text{K, Tl}$ ) to map out the boundaries of a high-field regime that was recently associated with the presence of the bulk quantum Hall effect. The phase inversion effect observed in the interplane magnetoresistivity and the behavior of quantum oscillations in the Hall potential are used to investigate the high-field region as a function of magnetic field, temperature, rotation angle, sweep rate, sample quality, and the anion of the charge-transfer salt. The inversion of the phase of the oscillations in  $\rho_{zz}$  is found to be directly related to the quality of the sample, and is suggested to be an intrinsic property of  $\alpha$ -(BEDT-TTF)<sub>2</sub>MHg(SCN)<sub>4</sub> ( $M = \text{K, Tl}$ ). A detailed mapping of the phase-inverted region indicates that its boundaries agree qualitatively with those of the recently proposed low-temperature-high-field state.

## I. INTRODUCTION

The high-magnetic-field properties of the quasi-two-dimensional organic charge-transfer salts  $\alpha$ -(BEDT-TTF)<sub>2</sub>MHg(SCN)<sub>4</sub> ( $M = \text{K, Tl}$ ) have attracted much attention.<sup>1–10</sup> The low-field, low-temperature states of these materials exhibit a complex behavior, and are thought to be density-wave (DW) states with complex Fermi surfaces (see Ref. 11 for a recent review). At fields above the so-called ‘‘kink’’ transition [marked by a sharp kink in the magnetoresistance occurring in the limit of low temperature at  $B_k \sim 23$  T for  $M = \text{K}$  (Refs. 12–15) and  $B_k \sim 25$  T for  $M = \text{Tl}$  (Ref. 16)], the Fermi surface (FS) is thought to consist of a quasi-two-dimensional (Q2D) hole pocket and a pair of quasi-one-dimensional (Q1D) electron sheets.<sup>9,11,17,18</sup> In the purest samples, at  $\sim 40$  T, the Landau levels are sharply resolved with an energy separation of  $\hbar\omega_c \sim 2.0$  meV, compared with a broadening from quasiparticle scattering of  $< 0.1$  meV and an interplane bandwidth of  $< 0.2$  meV.<sup>6,19</sup>

Such sharply resolved Landau levels are one of the prerequisites for the observation of the quantum Hall effect (QHE).<sup>6,20</sup> It has been suggested that the second requirement

for the QHE, i.e., a mechanism for the pinning of the chemical potential between completely filled and empty Landau levels over extended intervals of field, is fulfilled by a background density of electronic states provided by the Q1D sheets of the FS.<sup>6,19,21</sup> Numerical calculations, taking into account the finite warping of the Q1D sheets, have predicted an oscillatory field dependence of the Hall resistivity,  $\rho_{xy}$ , with quantized plateaux in the vicinity of integer values of  $F/B$ ,<sup>21</sup> where  $F$  is the fundamental frequency of the Landau quantum oscillations. With rising magnetic field, an increased localization of the Q1D carriers might be expected,<sup>21,22</sup> leading to a situation equivalent to that in 2D semiconductor systems. Some support for these proposals has come from the observation of plateaux in  $\rho_{xy}$  in the  $M = \text{Tl}$  salt in steady magnetic fields between 28 and 33 T.<sup>2</sup> It was suggested that the relative phase of the oscillations in  $\rho_{xy}$  and those in the measured in-plane resistivity  $\rho_{||} \approx \frac{1}{2}(\rho_{xx} + \rho_{yy})$  showed that there was some degree of localization of the Q1D carriers at such magnetic fields.<sup>2,21</sup>

A further remarkable phenomenon occurs at high fields and low temperatures in  $\alpha$ -(BEDT-TTF)<sub>2</sub>MHg(SCN)<sub>4</sub> ( $M = \text{K, Tl}$ ); quasipersistent induced in-plane currents are ob-

served at integer  $F/B$  in pulsed-field magnetization studies.<sup>1,3</sup> It has been suggested that these “eddy current resonances” are associated with deep minima in  $\rho_{||}$  which might be expected to accompany the QHE.<sup>6</sup> The induced in-plane currents exhibit saturation or critical currentlike behavior in pulsed-field magnetization<sup>1,3</sup> and Hall potential measurements.<sup>5</sup>

The fact that the bulk electronic density of states of the  $\alpha$ -(BEDT-TTF)<sub>2</sub>MHg(SCN)<sub>4</sub> ( $M=K, Tl$ ) salts at high magnetic field consists of widely-separated Landau levels with Q1D states, possibly partly localized, in between suggests that surface effects may become important. With increasing magnetic field and falling temperature, interplane transport through the bulk of the sample is expected to approach a regime where conduction is very much lower whenever the chemical potential  $\mu$  lies between two widely separated Landau levels. This leads to sharp peaks in the interplane magnetoresistivity  $\rho_{zz}$  at integer filling factors.<sup>19,23</sup> However, in a multilayered conductor with very sharply defined Landau levels, a chiral surface metal is expected to form at the edges of the sample through hybridization of the edge states associated with each layer.<sup>24–26</sup> The chirality arises from the fact that electrons can travel only along one direction perpendicular to the field, thereby suppressing any backscattering events.<sup>24,25</sup> At fields when the bulk of the sample will have low conductivity, these surface states should remain extended and dominate the conduction perpendicular to the layers, lowering the sharp maxima in  $\rho_{zz}$ . This effect has been demonstrated in semiconductor superlattices.<sup>27</sup> When  $\mu$  resides within a Landau level, the surface states are coupled to the bulk, as states in the interior of the sample, into which they can scatter, become available. Therefore, the effect of the so-called chiral Fermi liquid at the sample edges<sup>24,25</sup> on the longitudinal conduction is only observable at integer  $F/B$ .

In both  $\alpha$ -(BEDT-TTF)<sub>2</sub>KHg(SCN)<sub>4</sub> (Ref. 3) and  $\alpha$ -(BEDT-TTF)<sub>2</sub>TlHg(SCN)<sub>4</sub>,<sup>4,5,28</sup> experiments in steady and pulsed magnetic fields have shown a suppression of the maxima in the interplane resistivity  $\rho_{zz}$  with decreasing temperature,<sup>29</sup> even leading to a phase inversion of the oscillations in the highest-quality samples<sup>3,4</sup>; elsewhere,<sup>7</sup> “nodes” were observed in  $\rho_{zz}$  at certain temperatures and fields. In Ref. 3, it was shown that while the values of  $\rho_{zz}$  at integer  $F/B$  are strongly reduced, the temperature dependence at odd half-integer  $F/B$  is similar to that expected in conventional bulk interplane transport. It was concluded that the mechanism suppressing the amplitude of  $\rho_{zz}$  is chiefly operational when  $\mu$  lies between Landau levels<sup>3</sup>; this was interpreted as the bypassing of bulk interplane current paths by highly conducting surface states at the edges of the sample.<sup>3,4</sup> The amplitude reduction of  $\rho_{zz}$  was shown to take place only in samples which also exhibited plateaux in the Hall resistivity and/or eddy current resonances in the magnetization (see Refs. 1–3 and 30, and this work; sample B of Ref. 2 is identical to sample B,  $M=Tl$ , of this work), over the same field and temperature range where the latter effects were observed. Consequently, the suppression of the maxima in  $\rho_{zz}$  was linked to the proposed presence of the QHE.<sup>3</sup>

For a comprehensive study, it is important to have a detailed knowledge of the in-plane components of the resistivity tensor up to the highest magnetic fields. However, in

materials with a high intraplane/interplane anisotropy, it can prove very difficult to avoid the admixture of a dominant interplane component to an in-plane resistance signal.<sup>2,31</sup> In  $\alpha$ -(BEDT-TTF)<sub>2</sub>MHg(SCN)<sub>4</sub> ( $M=K, Tl$ ), this has so far ruled out measurements of  $\rho_{xy}$  and  $\rho_{||}$  in pulsed magnetic fields.<sup>2,4</sup> However, these problems can be overcome by utilizing the induced eddy currents, characteristic of a pulsed-magnetic-field experiment, as the driving current of the in-plane resistance measurement. In contrast to experiments where the current is applied externally, an inductive, wireless provision ensures that current flows entirely within the layers, and keeps the measured voltage free from any unwanted interplane component.<sup>5</sup> Using a Corbino-type geometry, this allows the Hall potential  $V_H$  between the center and periphery of the sample to be measured. For a cylindrical sample of radius  $a$ ,  $V_H$  is given by<sup>5</sup>

$$V_H \approx a^2 \frac{\partial B}{\partial t} \frac{\rho_{xy}}{\rho_{||}}. \quad (1)$$

Such experiments can be used to study the ratio  $\rho_{xy}/\rho_{||}$ , which is otherwise difficult to obtain experimentally.<sup>32</sup> Within the proposed quantum Hall regime, the Hall potential energy  $eV_H$  was found to be limited by the cyclotron energy  $\hbar\omega_c$ ,<sup>1,3,5</sup> leading to a current saturation at sweep rates typically achieved in pulsed magnetic fields and a concomitant enhancement of  $\rho_{||}$ .<sup>5</sup> This can be observed as a marked non-linearity in the dependence of  $V_H$  on the sweep rate  $\partial B/\partial t$ , and indicates a non-Ohmic  $I$ - $V$  characteristic of the sample.

While the proposed existence of the QHE in the  $\alpha$ -(BEDT-TTF)<sub>2</sub>MHg(SCN)<sub>4</sub> ( $M=K, Tl$ ) salts is still controversial, there is no doubt that several intriguing phenomena (the eddy-current resonances, the saturation of the induced currents and Hall potential, and the suppression of the maxima in  $\rho_{zz}$ ) occur simultaneously in low-temperature, high-field magnetotransport data; in what follows, we shall refer to these phenomena collectively as “anomalous magnetotransport.” In the pursuit of a theoretical understanding of these materials, it is desirable to discover the prerequisites for this anomalous behavior. Therefore, in this paper, we use the suppression of the maxima in  $\rho_{zz}$  and the saturating behavior of the Hall potential  $V_H$  in pulsed magnetic fields to map the  $B$ - $T$ - $\theta$ - $\tau$  space (here  $\theta$  is the angle between the normal to the Q2D planes and the field, and  $\tau^{-1}$  is the quasiparticle scattering rate) over which the anomalous magnetotransport effects are observed. Where appropriate, we shall point out aspects of the behavior which are consistent with the presence of the QHE.

## II. EXPERIMENTAL DETAILS

Measurements of the interplane magnetoresistance and the Hall potential were carried out in pulsed magnetic fields of up to 60 T, temperatures between 400 mK and 15 K, tilt angles  $\theta$  of up to 90° and sweep rates between 10<sup>3</sup> and 10<sup>4</sup> T/s, for a variety of samples of both the  $M=K$  and  $Tl$  compounds. The samples used in the present study (samples A, B, and C of the  $M=K$  salt and samples A and B of  $M=Tl$ ) were taken from the same high-quality batches used in Refs. 1–3 and 5. All crystals were of similar dimensions  $\sim 1.5 \times 1.5 \times 0.1$  mm<sup>3</sup>.

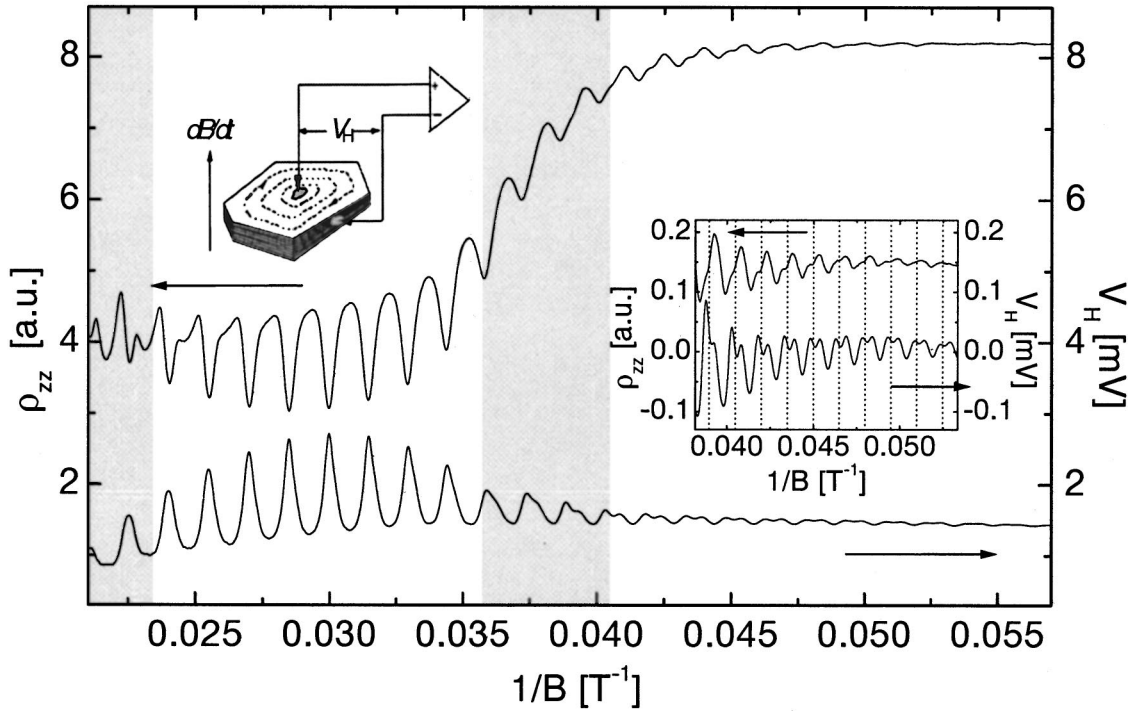


FIG. 1. Comparison of  $\rho_{zz}$  and  $V_H$  at  $T=0.5$  K in  $\alpha$ -(BEDT-TTF) $_2$ TIHg(SCN) $_4$ , with the field oriented normal to the conducting planes ( $\theta=0^\circ$ ); shaded regions denote where the oscillation phase inverts. The inset on the right shows the oscillatory components of  $\rho_{zz}$  and  $V_H$  within the low-field phase; vertical lines indicate fields at which the chemical potential lies exactly between Landau levels. The schematic on the top left shows the experimental configuration. For clarity, only the contact arrangement used to measure  $V_H$  is drawn; dashed curves indicate electric field lines for positive  $\partial B/\partial t$ . Two additional pairs of contacts (not shown) are placed on opposite faces of the crystal to measure  $\rho_{zz}$ .

The magnetoresistance was recorded using a fast lock-in amplifier operating at a frequency of 511.8 kHz. The sampling time was set to 2  $\mu$ s. Voltage and current contacts were placed on opposite sides of the crystals' (a,c) faces, and standard four-terminal techniques were used. The resistance was measured along the  $z$  axis, i.e., perpendicular to the highly conducting planes; for  $\theta=0$ , this direction is parallel to the magnetic-field vector (cf. Fig. 1). The contacts were applied using graphite paint and had typical two-point resistances of  $\sim 10$ – $20$   $\Omega$ . A variety of sample currents up to 100  $\mu$ A was used; care was taken to ensure that the applied current did not lead to sample heating. Control measurements were carried out at different lock-in frequencies to ensure that the observed effects were independent of measuring frequency. dc experiments showed an admixture of a Hall voltage component,<sup>33</sup> so that in this case the interplane resistance signal could only be obtained after subtracting forward and reverse current traces. We therefore note that ac techniques are to be preferred for reliable measurements of the resistance in pulsed magnetic fields.

For Hall potential measurements, two voltage contacts were placed on the sample in an adaptation of the Corbino geometry.<sup>5</sup> This configuration usually consists of a pair of ring contacts, one about a hole in the center, and the other around the edges of the sample. However, since samples of  $\alpha$ -(BEDT-TTF) $_2$ MHg(SCN) $_4$  ( $M=K, Tl$ ) are of a nonideal shape, one contact has been placed on the center of the top surface and one at the edge (see Fig. 1); a high-impedance preamplifier was used to record the voltage. The crystals were mounted such that measurements of  $\rho_{zz}$  and  $V_H$  could

be carried out on successive shots, with the sample remaining *in situ*, ensuring that the same external parameters applied.

Pulsed magnetic fields of up to 60 T with a rise time of  $\sim 10$  ms were provided by the Los Alamos National High Magnetic Field Laboratory (Refs. 34 and 35); plastic  $^3$ He and  $^4$ He refrigerators were used to obtain temperatures between 0.4 and 15 K. A plastic one-axis rotator based on a wormdrive mechanism with an accuracy greater than  $0.5^\circ$  was purpose built for the rotation experiments.

### III. RELATIVE PHASE OF OSCILLATIONS IN $\rho_{zz}$ AND $V_H$

Figure 1 compares the oscillations of the interplane magnetoresistivity  $\rho_{zz}$  and the Hall potential  $V_H$  in a sample of  $\alpha$ -(BEDT-TTF) $_2$ TIHg(SCN) $_4$ , which will be referred to as sample A. The traces are plotted against reciprocal field at a temperature of  $T=0.5$  K and at  $\theta=0$ . According to bulk magnetotransport theory,<sup>19,23</sup>  $\rho_{zz}$  is expected to display maxima at integer values of  $F/B$ , and therefore to oscillate in phase with  $V_H \propto \rho_{xy}/\rho_{||}$ .<sup>2,5,21</sup> At the highest fields shown in Fig. 1,  $\rho_{zz}$  is roughly in phase with  $V_H$ , and both exhibit maxima at integer values of  $F/B$ . However, at  $\sim 44$  T,  $\rho_{zz}$  displays what might loosely be termed a “node” at  $T=0.5$  K (Fig. 1); over a region of field below this (the region between the two gray shaded areas in Fig. 1) the oscillations in  $V_H$  and  $\rho_{zz}$  are in antiphase. Figure 2 shows that the node (indicated by gray shading) shifts to lower fields at higher temperatures; at fields above the node,  $\rho_{zz}$  exhibits maxima

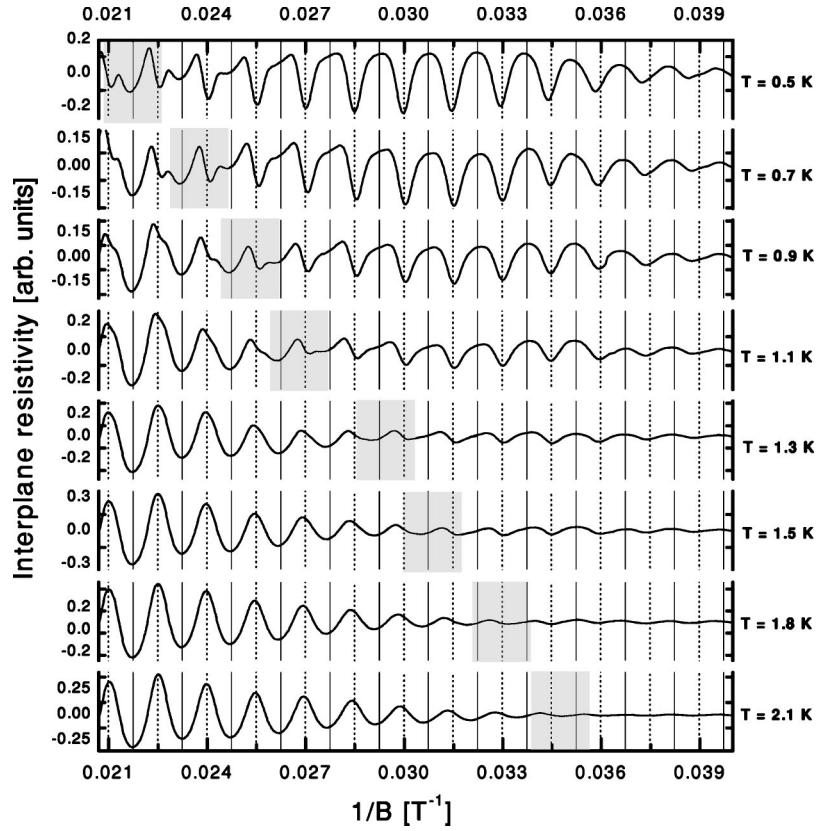


FIG. 2. Background-removed traces of  $\rho_{zz}$  within the high-field region at  $\theta=0^\circ$  for a variety of temperatures. The dotted lines indicate integer values of  $F/B$ , the solid lines odd half-integer values of  $F/B$ . The shaded regions denote a phase change of  $\Delta\phi=\pi$ .

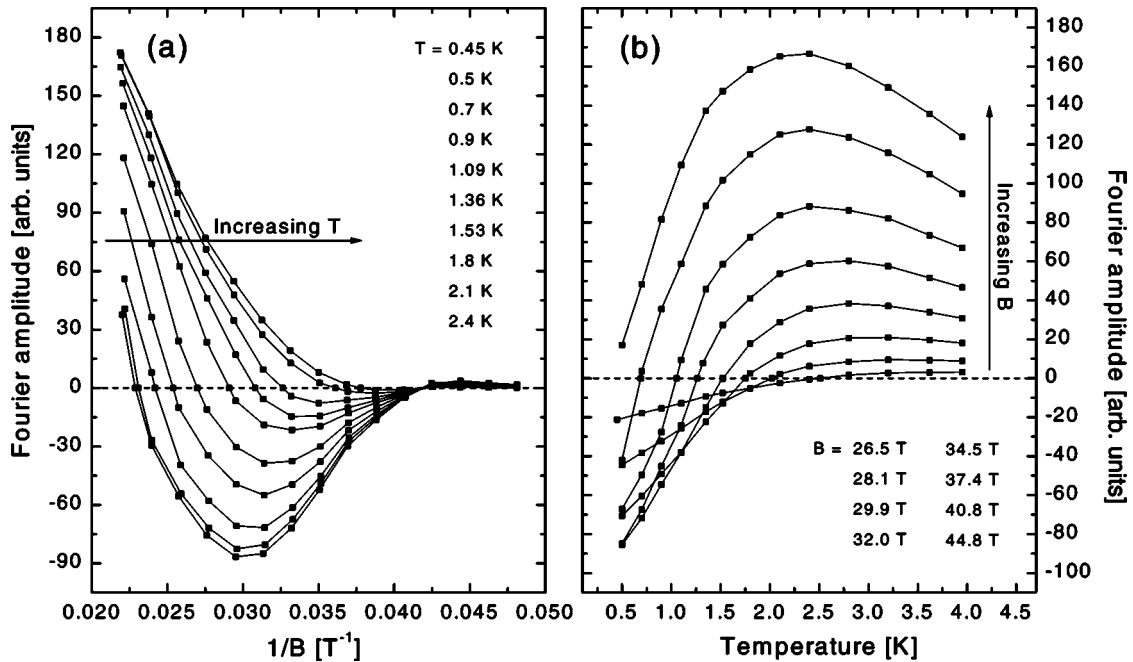


FIG. 3. (a) Field dependence of the Fourier amplitude of the oscillations in  $\rho_{zz}$  at temperatures between  $T=0.45$  and  $2.4$  K at  $\theta=0^\circ$ ; the Fourier amplitude has a positive sign if the oscillations exhibit maxima at integer  $F/B$ , and a negative sign if they have minima. (b) Temperature dependence of the Fourier amplitude at  $\theta=0^\circ$  at a variety of magnetic fields above the kink transition; the field indicated is the reciprocal of the midpoint of the Fourier window over which the transform was performed.

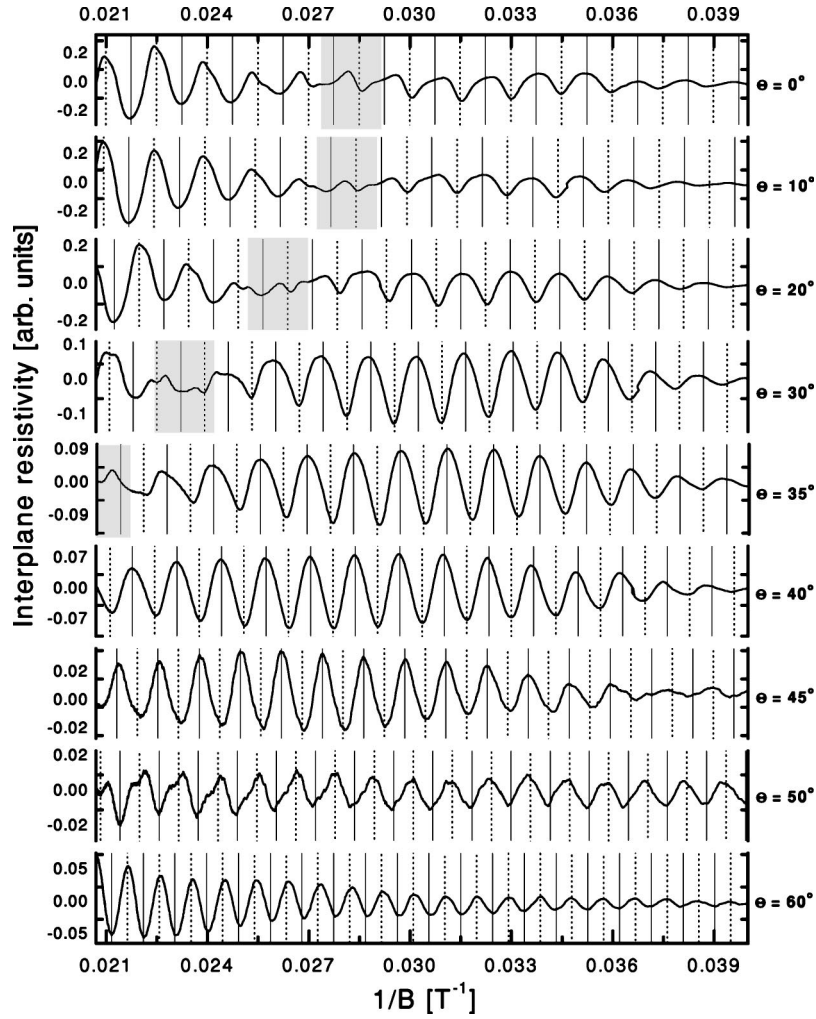


FIG. 4. Background-removed traces of  $\rho_{zz}$  within the high-field region at a variety of angles at  $T=1.2$  K; dotted lines indicate integer  $F/B$ , solid lines odd half-integer  $F/B$ . The shaded regions denote a phase change of  $\Delta\phi=\pi$ .

at integer  $F/B$  (dotted lines), in agreement with the expectations of transport theory,<sup>19,23</sup> while at fields below it,  $\rho_{zz}$  has *minima* at integer  $F/B$ .<sup>40</sup> As mentioned above, the presence of these minima in  $\rho_{zz}$  at integer  $F/B$  has been attributed to the presence of edge states which ‘‘short circuit’’ the current paths through the bulk of the sample.<sup>3,4</sup> The node, occurring at a temperature-dependent field which we shall denote as  $B_{inv}$ , may thus be said to form a high-field limit of the anomalous magnetotransport behavior. Note that over the field range at which the node is occurring (see Fig. 2), the oscillation phase of  $V_H$  remains unchanged, precluding the possibility that the node may be due to beating, arising, for example, from an area difference between the neck and belly orbit of the Q2D FS cylinder.

The right-hand shaded region in Fig. 1 ( $\sim 24.5$  T  $< B < 28$  T,  $\rho_{zz}$ ) indicates the field range where large hysteresis in the resistivity occurs between upsweeps and downsweeps of the magnetic field,<sup>2,8,13</sup> and where a change in the slope of Dingle plots<sup>8,9,36–39</sup> has been observed; all are associated with the ‘‘kink’’ transition from the low-field, low-temperature state. The transition region is thought to be spread out due to the influence of the oscillatory part of the chemical potential,  $\tilde{\mu}$ , which becomes comparable to the DW order parameter, and induces a series of first-order tran-

sitions between the two states.<sup>12</sup> At fields below this transition region, the oscillations  $V_H$  and  $\rho_{zz}$  in this sample appear to possess the same phase (Fig. 1, inset). However, the quantum oscillations in the low-field, low-temperature phase are greatly complicated by a pronounced splitting, ascribed to a dominant  $2F$  frequency in the free energy, caused by the effect of  $\tilde{\mu}$  on the width of the DW gap.<sup>11,12</sup>

The changes in phase can also be detected using Fourier analysis. In Fig. 3(a), the field dependence of the Fourier amplitude<sup>40</sup> of the fundamental frequency  $F_\alpha=667$  T of the Q2D FS orbit is plotted for a variety of temperatures, with the phase information of the transform retained. The phase of the transform is set using data at fields above the kink as follows; the Fourier amplitude is taken to be *positive* if  $\rho_{zz}$  is higher at integer  $F/B$  than at half-integer  $F/B$ , whereas the Fourier amplitude is taken to be *negative* if  $\rho_{zz}$  is lower at integer  $F/B$  than at half-integer  $F/B$ . Therefore, at high temperatures, where the data are in agreement with theories of magnetotransport,<sup>19,23</sup> (i.e., before the anomalous transport sets in; see Fig. 2) the amplitude is positive. When the anomalous transport occurs, the peaks in the oscillations get eaten away,<sup>3,4</sup> until  $\rho_{zz}$  at these fields can be lower than that at half-integer  $F/B$  (see Fig. 2). At this point, the amplitude will become negative; previous works have associated such

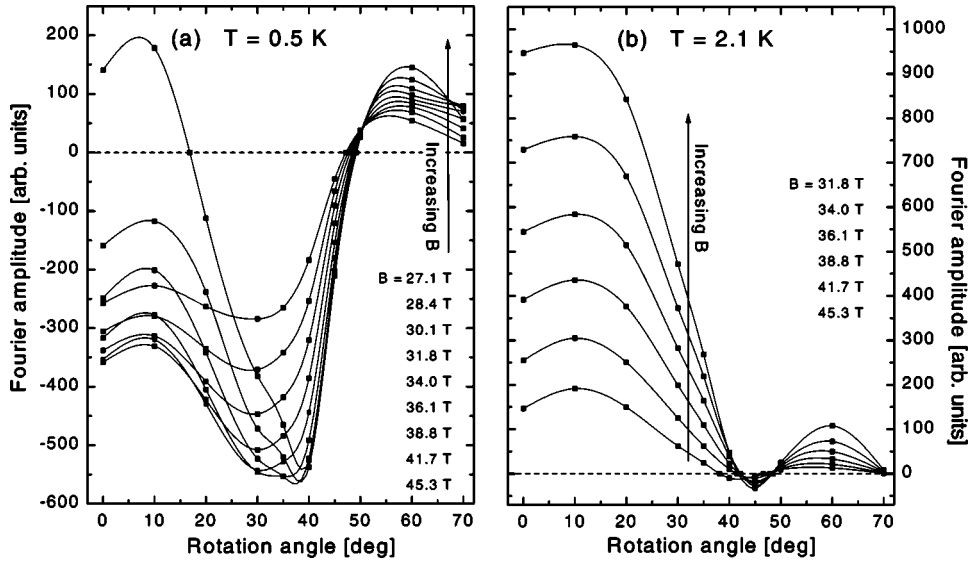


FIG. 5. Phase-sensitive plots of the angle dependence of the Fourier amplitude of  $\rho_{zz}$  at different fields for (a)  $T=0.5$  K and (b)  $T=2.1$  K. The data points have been connected by spline curves.

negative Fourier amplitudes with the presence of the highly efficient surface conduction mechanism.<sup>3,4</sup>

Figure 3(a) shows that the interval in reciprocal field over which large negative amplitudes occur decreases with increasing temperature; i.e.,  $B_{\text{inv}}$  is converging towards the field of the kink transition  $B_k$  with increasing temperature. Thus the greatest relative reduction of the amplitude of the  $\rho_{zz}$  oscillations takes place soon above the transition into the high-field state at  $B_k$ , in contrast to assumptions of previous works,<sup>3,4</sup> which proposed that this was the case at the highest fields. Figure 3(b) emphasizes that the presence of the anomalous magnetotransport region produces a temperature dependence of the  $\rho_{zz}$  oscillations which is very different from the expectations of the conventional Lifshitz-Kosevich formalism for quantum oscillations,<sup>41</sup> showing that the application of such techniques to the analysis of magnetotransport data from  $\alpha\text{-(BEDT-TTF)}_2\text{MHg(SCN)}_4$  ( $M=K, \text{TI}$ ) at high fields is of dubious utility.

In addition to its dependence on temperature,  $B_{\text{inv}}$  also changes with rotation angle  $\theta$  between the direction of the magnetic field and the normal to the conducting planes. Figure 4 shows the development of the oscillatory component of  $\rho_{zz}$  (Ref. 40) with angle  $\theta$  at a temperature of  $T=1.2$  K. The inversion field  $B_{\text{inv}}$  moves toward higher fields with increasing angle, and is eventually pushed out of the available field range for  $\theta > 35^\circ$ .

Complementary information can be gained by investigating the angle-dependence of the Fourier amplitude within the high-field state (Fig. 5). At  $T=0.5$  K [Fig. 5(a)], the oscillation phase is inverted, for all but the highest-field trace, at all angles up to  $\theta \sim 47^\circ$ . As the temperature is increased, the data revert back to positive amplitudes; at  $T=2.1$  K [Fig. 5(b)], the interplane transport appears to have a positive Fourier amplitude at all fields for  $\theta < 40^\circ$ . As for  $T=0.5$  K, the Fourier amplitude becomes positive again at  $\theta \sim 47^\circ$ . However, this second sign change can be associated with a spin splitting zero, occurring whenever the spin reduction factor  $R_s = \cos[\pi g^*(m^*/m_e)/2]$  of the oscillation amplitude equals zero<sup>41</sup>;  $g^*$  denotes the effective Landé  $g$  factor,  $m^*$  the qua-

siparticle effective mass, and  $m_e$  the free-electron mass. Owing to the Q2D nature of  $\alpha\text{-(BEDT-TTF)}_2\text{TIHg(SCN)}_4$ ,  $m^*$  scales with  $1/\cos \theta$  as the angle is increased,<sup>42</sup> so that the condition for a spin-zero is given by

$$g^* \frac{m^*(0^\circ)}{m_e} \frac{1}{\cos \theta} = 2s + 1, \quad (2)$$

where  $s$  is an integer. The first spin-zero can be realized for  $s=2$  and with  $\theta_2 = (47 \pm 2)^\circ$ ; this yields  $g^* m^*(0^\circ)/m_e = 3.4 \pm 0.1$ . This compares with a value of 3.63 obtained for the  $M=K$  compound.<sup>43</sup> Using  $m^* \sim 1.8 m_e$ ,<sup>3,38,44</sup> an effective  $g$  factor of  $1.9 \pm 0.1$  can be derived. Further spin zeros are expected for angles  $\theta_s \sim 61^\circ, 68^\circ, 72^\circ, \dots$ , but can not be resolved in our measurement due to the limited amount of

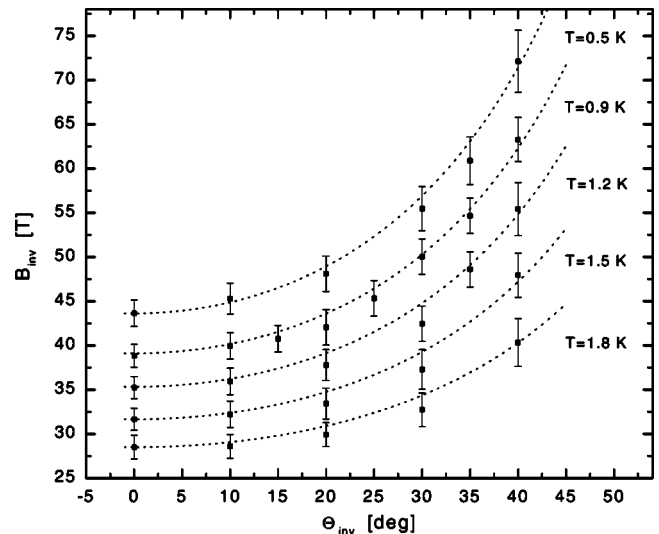


FIG. 6. Angle dependence of the upper inversion field  $B_{\text{inv}}$  for temperatures between 0.5 and 1.8 K. The dotted lines are fits to the data of the function  $B_{\text{inv}}(\theta) = B_{\text{inv}}(0^\circ)/(\cos \theta)^n$ ;  $n$  is a fit parameter and was determined to be  $\sim 1.85, 1.75, 1.65, 1.5,$  and  $1.3$  for  $T = 0.5, 0.9, 1.2, 1.5,$  and  $1.8$  K, respectively.

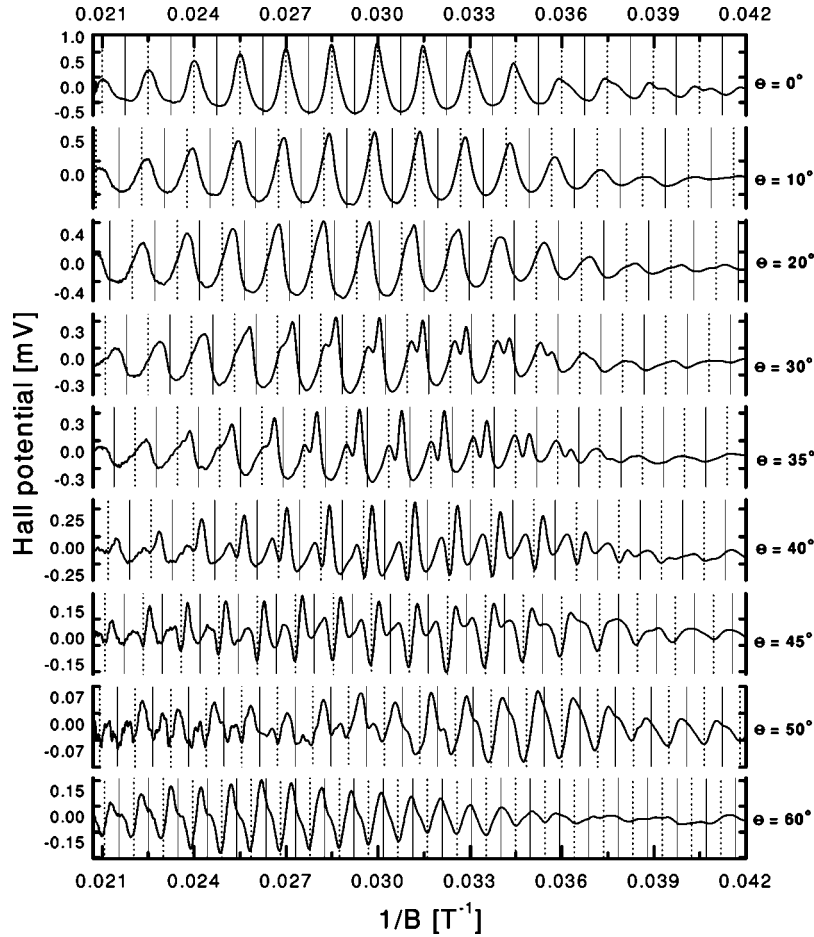


FIG. 7. Oscillatory part of the Hall potential  $V_H$  at  $T=0.5$  K, plotted against the reciprocal field for a variety of angles  $0^\circ \leq \theta \leq 60^\circ$ ; the dotted lines indicate integer  $F/B$ , and the solid lines odd half-integer  $F/B$ .

data in this angle range. The strong second harmonic content at  $\theta=50^\circ$  in Fig. 4, which becomes more pronounced at lower temperatures, can therefore be attributed to Zeeman spin splitting, in contrast to that of the oscillations within the low-field phase (cf. Fig. 1).

Virtually all previous work links the observation of anomalous magnetotransport phenomena with the establishment of very well-resolved Landau levels.<sup>3,4,6</sup> Following this reasoning, the lower boundary field  $B_l$  for entry into the region in which anomalous magnetotransport occurs should depend largely on the establishment of a suitably large energy separation  $\hbar\omega_c$  between adjacent Landau levels. Since  $\hbar\omega_c$  decreases with  $\cos\theta$  as the angle is increased,  $B_l(\theta)$  is expected to scale with  $1/\cos\theta$ . For each magnetic field  $B$ , there is then a limiting angle  $\theta_l$  at which  $\hbar\omega_c$  becomes too small. This should be observable as a further zero crossing of the Fourier amplitude. However, for the temperatures shown in Fig. 5, this does not appear to be the case for  $\theta < 50^\circ$ , above which the resolution becomes too low. We can hence estimate an upper limit for  $B_l(0^\circ)$  at  $T=0.5$  K, using numbers from Fig. 5(a):  $B_l(0^\circ) \sim \cos\theta \times B_l(\theta) < \cos 50^\circ \times 27.1$  T = 17.5 T  $< B_k$ . However, as a consequence of its reconstruction in the low-field, low-temperature state, the FS topology becomes much more complex below  $B_k$ ,<sup>11</sup> so that in practice,  $B_k \sim 25$  T seems to be the lower limiting field for the observation of the anomalous magnetotransport.

Figure 6 shows the angle dependence of  $B_{\text{inv}}$  derived from

data such as those in Fig. 3; the values of  $B_{\text{inv}}$  correspond to the zero crossings of the Fourier amplitude of  $\rho_{zz}$ .<sup>45</sup> The angle dependence of  $B_{\text{inv}}$  varies with temperatures; the dotted lines in Fig. 6 correspond to fits of the form  $B_{\text{inv}}(\theta) = B_{\text{inv}}(0^\circ)/(\cos\theta)^n$ , using the power  $n$  as a fit parameter;  $n$  increases from a value of  $\sim 1.3$  at  $T=1.8$  K to  $n \sim 1.85$  at  $T=0.5$  K.

In models which associate the anomalous behavior of  $\rho_{zz}$  with the presence of surface conducting paths,  $B_{\text{inv}}$  would represent the field at which the oscillations in  $\rho_{zz}$  revert back to a mode which can be described by bulk interplane transport.<sup>19,23</sup> In such a picture, any mechanism which led to a return to bulk conduction would also suppress the QHE at a similar field. In Ref. 5, it was proposed that a degradation of the suggested QHE could be caused by the onset of magnetic breakdown between the Q1D and Q2D sections of the FS (one might regard this as the fragmentation of the simple electronic density of states, composed of widely spaced Landau levels plus a slowly varying background from the Q1D states, into a plethora of magnetic breakdown levels). If this were the case, one might expect  $B_{\text{inv}}$  to be related to a critical field  $B_c$  at which the magnetic breakdown probability reached some value  $P_c$  sufficient to destroy the QHE. Assuming that  $P_c = e^{-B_0/B_c}$  is independent of angle in a first approximation,  $B_c$  might be expected to scale in the same way as the magnetic breakdown field  $B_0$ , which will be pro-

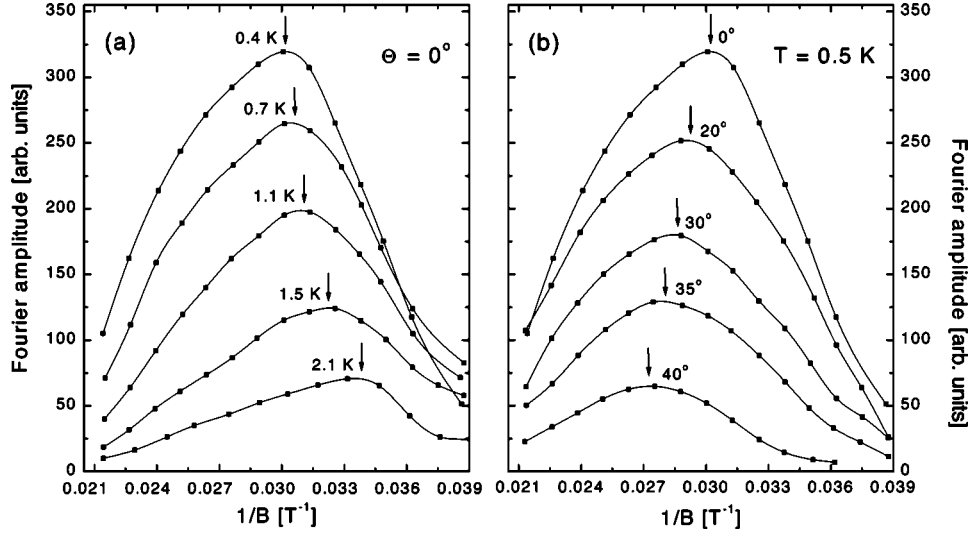


FIG. 8. Field dependence of the Fourier amplitude of the fundamental frequency of  $V_H$  for (a) a variety of temperatures at  $\theta=0^\circ$  and (b) a variety of angles at  $T=0.5$  K. The Fourier window was taken over the high-field region. The data points were connected by spline functions; arrows indicate local maxima.

portional to  $1/\cos\theta$  in a simple Q2D model.<sup>41</sup> As noted above,  $B_{\text{inv}}$  in fact follows a rather faster variation with  $\theta$ , which also depends on temperature, showing that such a model is at the very least an oversimplification.

#### IV. OSCILLATIONS OF THE HALL POTENTIAL

We now turn to the quantum oscillations of the Hall potential of  $\alpha$ -(BEDT-TTF)<sub>2</sub>TlHg(SCN)<sub>4</sub>. Figure 7 shows Hall potential data from which the slowly varying magnetoresistance background has been subtracted for angles between  $0^\circ$  and  $60^\circ$  (sample A at  $T=0.5$  K). At all fields and for  $\theta < 40^\circ$ , the oscillations exhibit maxima when  $\mu$  lies between Landau levels, as is expected from the proportionality of  $V_H$  with  $\rho_{xy}/\rho_{\parallel}$ .<sup>5</sup> With increasing angle, a very strong

second harmonic content appears, and dominates the oscillatory wave form at angles between  $30^\circ$  and  $50^\circ$ . The positions of the maxima and minima invert between  $40^\circ$  and  $50^\circ$ . This agrees with the observation of a spin-splitting zero in the interplane resistivity within the same angle range (cf. Fig. 5).

The amplitude of the Hall potential oscillations is expected to be strongly dependent on whether the sample is within the anomalous magnetotransport regime. As summarized in Sec. I, within this regime it appears that deep minima in  $\rho_{\parallel}$  lead to sharp maxima of  $V_H$  at integer  $F/B$ . Pulsed-magnetic-field measurements of  $\alpha$ -(BEDT-TTF)<sub>2</sub>TlHg(SCN)<sub>4</sub> (Ref. 5) have shown that these maxima are truncated as  $eV_H$  becomes comparable to the cyclotron energy  $\hbar\omega_c$ . As one leaves the anomalous region, however, the minima in  $\rho_{\parallel}$  are expected to rise sharply,

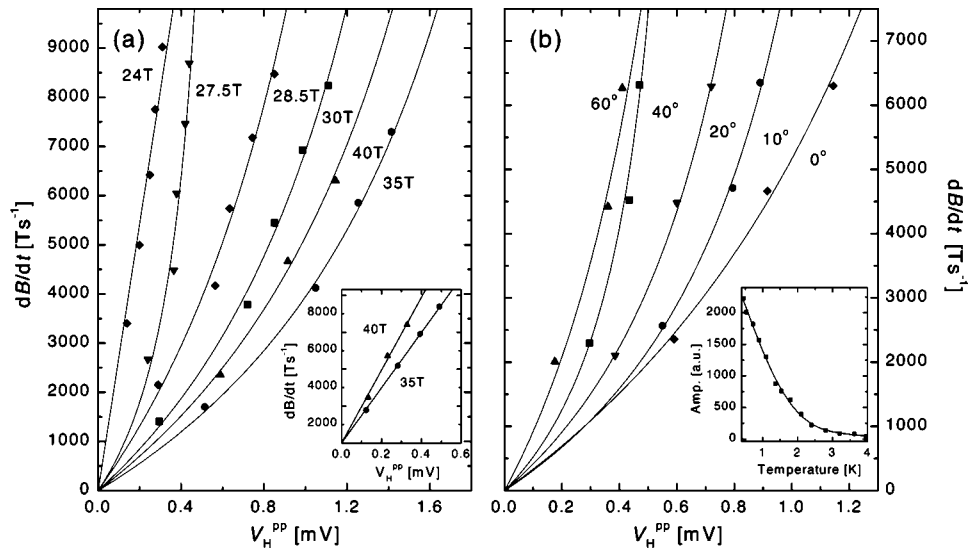


FIG. 9. (a) Peak-to-peak amplitude  $V_H^{\text{pp}}$  of the oscillations in  $V_H$  plotted against  $\partial B/\partial t$  for a variety of fields  $B$  below and above the kink transition. The solid lines are fits of the data to the function  $V_H^{\text{pp}} = \gamma(\partial B/\partial t)V_H^{\text{lim}}/[\gamma(\partial B/\partial t) + V_H^{\text{lim}}]$  for  $B \geq 27.5$  T;  $\gamma$  and  $V_H^{\text{lim}}$  are fit parameters; the fit for  $B = 24$  T is linear. The fits merely act as guides to the eye. Inset:  $V_H^{\text{pp}} - \partial B/\partial t$  dependence at  $T = 1.5$  K for  $B = 35$  and 40 T. The solid lines are linear fits. (b) Plots at  $T = 0.5$  K for a variety of angles  $0^\circ \leq \theta \leq 60^\circ$ . The solid lines are fits of the data as in (a). Inset: temperature dependence of the Fourier amplitude of  $V_H$  at  $\theta = 0^\circ$ ; the solid line is a least-square fit.



leading to a reduction of the maxima of  $V_H$ .<sup>5</sup> A turning point in the oscillation amplitude of  $V_H$  may therefore be used as a means of delimiting the anomalous region.

Figure 8 shows the development of the field dependence of the Fourier amplitude of  $V_H$  both for increasing temperature and rotation angle. It can be seen that the position of the maximum Fourier amplitude moves down in field with increasing temperature and up in field as the angle increases. Hence the maximum Hall potential amplitude  $V_{H,\max}$  behaves in an equivalent fashion to the field  $B_{\text{inv}}$  as a function of temperature and angle. It should be noted that the two techniques described to probe the state of the sample are completely independent of each other, but both yield similar limits for the anomalous magnetotransport region.

Apart from factors of proportionality, the  $I$ - $V$  characteristics of the sample can be seen by plotting the peak-to-peak amplitude  $V_H^{pp}$  of the oscillations in  $V_H$  against the sweep rate  $\partial B/\partial t$  (Ref. 5); the circulating current  $I = V_H/\rho_{xy}$  ( $\rho_{xy}$  is constant at fixed field and temperature) and the driving electromotive force  $V \propto \partial B/\partial t$ . A nonlinear dependence indicates the saturation of the induced current, a phenomenon associated with the anomalous magnetotransport regime; this has been interpreted in connection with the breakdown of the QHE.<sup>1,3,5</sup> An Ohmic dependence at pulsed-field sweep rates, on the other hand, suggests that one is outside the anomalous region. Figure 9(a) shows the  $V_H^{pp} - \partial B/\partial t$  dependence of sample A for a variety of fields below and above the kink transition at a temperature of  $T = 0.5$  K. Sweep rates between 1000 and 10000 T/s were generated by changing the voltage to which the capacitor bank was charged.<sup>34,35</sup> It can be seen that while the dependence is nonlinear for all fields above the kink transition, it is Ohmic for  $B \sim 24$  T. This supports the earlier suggestion that the anomalous magnetotransport region is only established for fields  $B > B_k$ . The largest nonlinearity is observed for  $B \sim 35$  T. The fact that the features become less pronounced at  $B \sim 40$  T is consistent with the measurements of  $\rho_{zz}$  reported in Sec. III (cf. Fig. 1). At  $T = 1.5$  K and  $\theta = 0^\circ$  [see the inset to Fig. 9(a)], the  $I$ - $V$  characteristics for 35 and 40 T are Ohmic. This is consistent with Fig. 6, which shows that the upper phase inversion field  $B_{\text{inv}}$  at  $T = 1.5$  K is  $\sim 32$  T. In Fig. 9(b), the angle dependence of  $V_H^{pp}$  against  $\partial B/\partial t$  up to  $\theta = 60^\circ$  is plotted at a temperature of  $T = 0.5$  K. All curves are nonlinear, which indicates a saturating-current-like behavior, indicative of the anomalous magnetotransport regime, for rotation angles up to  $60^\circ$ .

Finally, the inset to Fig. 9(b) shows the temperature dependence of the Fourier amplitude of  $V_H$ . The rise at low temperatures is much steeper than for other types of quantum oscillations previously observed in  $\alpha$ -(BEDT-TTF)<sub>2</sub>MHg(SCN)<sub>4</sub> ( $M = \text{K, TI}$ ).<sup>9,13,16,36,43</sup> If one were to naively fit the data to the Lifshitz-Kosevich formalism,<sup>41</sup> the slope would correspond to an effective mass of  $m^* \sim 5.3m_e$ . This, however, can be taken as an indication (recalling that  $V_H \propto \rho_{xy}/\rho_{\parallel}$ ) that the deep minima in  $\rho_{\parallel}$  are rapidly disappearing as the temperature rises.

## V. SAMPLE DEPENDENCE

In this section, we present a systematic study of the occurrence of the anomalous magnetotransport in the interplane magnetoresistivity as a function of sample quality. The mea-

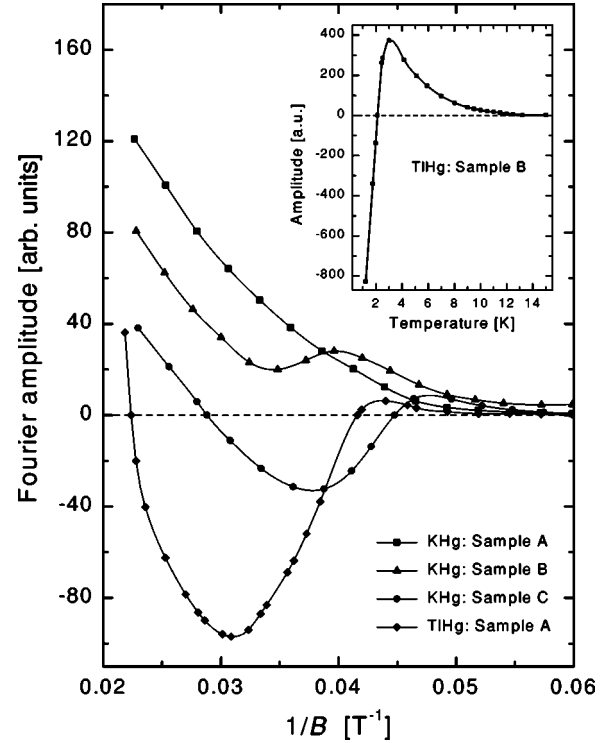


FIG. 10. Phase-sensitive plot of the field dependence of the Fourier amplitude of  $\rho_{zz}$  in samples A, B, and C of the  $M = \text{K}$  compound, and sample A of the  $M = \text{TI}$  compound;  $T = 0.5$  K,  $\theta = 0^\circ$ . Inset: temperature dependence of the  $\rho_{zz}$  Fourier amplitude of sample B,  $M = \text{TI}$ , for  $1.2 \text{ K} \leq T \leq 15 \text{ K}$ ; Fourier window:  $27 \text{ T} < B < 50 \text{ T}$ . The data points were connected by spline curves.

surements were conducted on three samples A, B, and C of the  $M = \text{K}$  compound and two samples A and B of the  $M = \text{TI}$  compound. Samples A, B, and C of the  $M = \text{K}$  salt were shown to have Dingle temperatures  $T_D$  of  $2.1 \pm 0.3$ ,  $1.7 \pm 0.1$ , and  $0.4 \pm 0.2$  K, respectively, within their high-field states. The Dingle temperatures of samples B and C were determined in pulsed-field magnetization studies, following the method described in Ref. 3.  $T_D$  of sample A was derived from fitting the Lifshitz-Kosevich formalism<sup>41</sup> to the resistance data, the applicability of which was warranted by the relatively low quality of the sample.<sup>19</sup> Sample A of the  $M = \text{TI}$  salt (the sample used in Secs. III and IV of the present study) was found to have a Dingle temperature of  $T_D = 0.6 \pm 0.2$  K, again derived from pulsed-field magnetization studies.  $T_D$  of sample B,  $M = \text{TI}$ , was not available as no magnetization experiments were carried out on this sample. It is, however, likely to have the overall highest quality, as quantum oscillations of up to a temperature of 15 K were observed (see the inset to Fig. 10).

Figure 10 shows a plot of the Fourier amplitudes of  $\rho_{zz}$  against reciprocal field at  $T = 0.5$  K. Samples A–C of the  $M = \text{K}$  salt exhibit a direct relationship between sample purity and the degree to which negative Fourier amplitudes are observed. The least pure sample, A, has a very conventional field dependence with its amplitude increasing monotonically with field. Sample B already displays a local minimum, while its Fourier amplitude remains positive. The purest sample, C, however, exhibits a negative Fourier amplitude over a field region of  $\sim 22.5 \text{ T} < B < 34.5 \text{ T}$ . An even larger

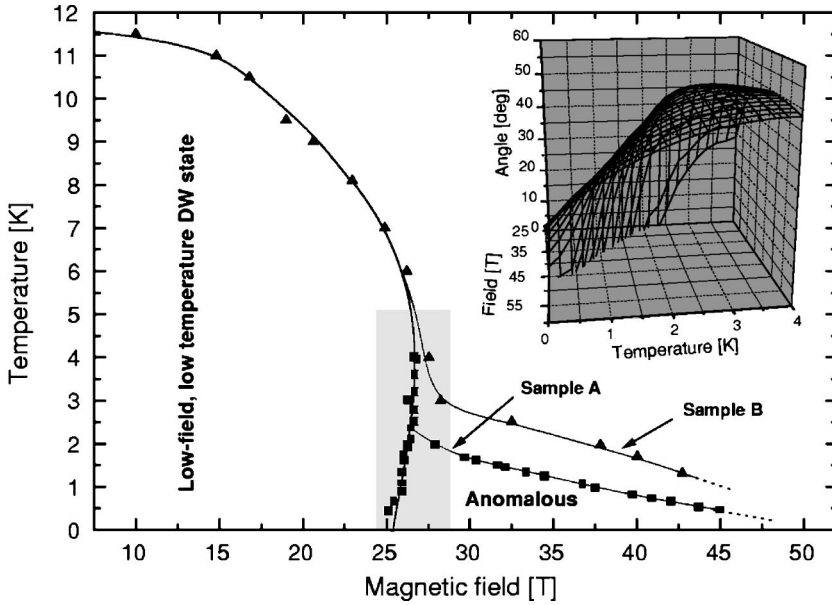


FIG. 11. Diagram mapping the “anomalous magnetotransport region.” The phase boundary of the low-temperature–low-field DW state has been determined by measuring the kink field  $B_k$  on downsweeps of the magnetic field. Filled squares indicate data points derived from  $\rho_{zz}$  traces of sample A; triangles correspond to sample B. The shaded area denotes the transition region between the DW and anomalous regime (see text). Inset: Three-dimensional diagram with the rotation angle plotted along the vertical axis; the data have been smoothed by adjacent averaging. The  $T$ - $\theta$  plane at  $B \sim 25$  T corresponds to the lower phase boundary at  $B_k$  (see the text).

interval in field ( $\sim 25 \text{ T} < B < 44 \text{ T}$ ) with reversed oscillation phase is observed for sample A of the  $M = \text{Tl}$  compound (see also Fig. 3). The different lower critical fields result from the different values of  $B_k$  in both salts.<sup>2,16,42</sup> Finally, sample B of  $M = \text{Tl}$ , shows the most pronounced effects. The inset to Fig. 10 shows a plot of its oscillation amplitude for a temperature of up to 15 K at  $\theta = 0^\circ$ ; the phase inversion temperature  $T_{\text{inv}}$  of 2.1 K is the highest thus far observed for a transform performed across the entire high-field region [cf. Fig. 3(b) of this work and Fig. 3 of Ref. 3].

In summary, the occurrence of the negative Fourier amplitude of the oscillations in  $\rho_{zz}$  (indicative of the anomalous magnetotransport effects) and the width of the field region across which the effect is realized are directly dependent on the purity of the sample. The measurements suggest that the anomalous magnetotransport region is intrinsic to  $\alpha$ -(BEDT-TTF)<sub>2</sub>MHg(SCN)<sub>4</sub> ( $M = \text{K}, \text{Tl}$ ) charge-transfer salts, and should also be observable in the  $M = \text{Rb}$  compound.<sup>29</sup> Its manifestation depends on sufficient sample quality for which we estimate a purity corresponding to a Dingle temperature of  $\leq 1$  K to be necessary.

These findings are consistent with proposals that interpret the anomalous magnetotransport region as a consequence of the QHE.<sup>6</sup> An increased quasiparticle scattering rate  $\tau^{-1}$  will lead to an increased broadening  $\hbar/\tau$  of the Landau levels. Since the Landau levels need to be sharply resolved for the QHE to be feasible, diminished sample quality will eventually rule out its observation. Thus only the cleanest samples exhibit the QHE and a concomitant enhancement of the edge state conductivity which is proposed to lead to the suppression of the maxima in  $\rho_{zz}$ .<sup>3</sup>

## VI. DIAGRAM OF THE ANOMALOUS MAGNETOTRANSPORT REGIME

The information gathered in the previous sections can be compiled to draw a diagram of the region in  $B$ - $T$  space over which the anomalous magnetotransport characteristics (relative phase inversion of  $\rho_{zz}$  and  $V_H$ , non-Ohmic behavior of  $V_H$ , etc.) occur. Figure 11 shows such a diagram for samples

A and B of  $\alpha$ -(BEDT-TTF)<sub>2</sub>TlHg(SCN)<sub>4</sub> at  $\theta = 0^\circ$ . The boundary of the low-temperature–low-field state was determined by measuring the kink field  $B_k$  on downsweeps of the magnetic field (cf. Refs. 13, 14, 16, 37, and 42). The two boundaries at higher fields delineate the change from anomalous to conventional oscillation mode in samples A and B, respectively. The shaded area in Fig. 11 represents the region of strong hysteresis between upsweeps and downsweeps of the magnetic field. In the higher-quality sample B,  $T_{\text{inv}}$  curves up to form a continuation of the boundary of the low-temperature, low-field state (the “kink” transition). With increasing field,  $T_{\text{inv}}$  decreases monotonically. For sample A, the upper boundary roughly extrapolates to  $B_{\text{inv}} \sim 49 \pm 4$  T at the intersection with  $T = 0$ . The boundary of sample B appears to curve down toward a similar limiting field, although more data are necessary to characterize the behavior at lower temperatures.

The inset to Fig. 11 shows a three-dimensional plot of the anomalous magnetotransport region of sample A. The rotation angle  $\theta$  is included and plotted along the vertical axis.  $B_k$  is almost independent of temperature and angle within the plotted range,<sup>46</sup> and corresponds to the  $T$ - $\theta$  plane at  $B_k \sim 25$  T. The region between this plane and the plotted surface therefore marks the regime where the anomalous magnetotransport behavior occurs. If one follows the proposals of Refs. 1–5 and 21, the same region can be associated with the occurrence of the QHE.

The thermodynamic phase diagram of  $\alpha$ -(BEDT-TTF)<sub>2</sub>MHg(SCN)<sub>4</sub> ( $M = \text{K}, \text{Tl}$ ) has been the subject of ongoing discussion.<sup>47</sup> While the phase boundary demarcating the low-temperature–low-field state is universally accepted, a more complicated phase diagram has been proposed outside this region.<sup>7,8,48–50</sup> However, there is still considerable debate as to the nature of the low-temperature–high-magnetic field region.<sup>7,8,18,48–54</sup> The common feature of models proposing a more complicated diagram<sup>7,8,48–50</sup> is a phase defined by a boundary adjoining onto the low-temperature, low-field state, extending toward higher magnetic fields and, in extrapolation, intersecting the  $T = 0$  axis somewhere between 40 and 60 T. A comparison with Fig. 11 shows that

this proposed low-temperature–high-magnetic-field state coincides with the region defined by the anomalous magnetotransport. However, while the lower boundary (at  $\sim B_k$ ) is found to be independent of sample, the upper boundary is strongly sample dependent, i.e., the area of  $B$ - $T$  space covered increases with the quality of the sample (see Figs. 10 and 11).

Following the proposal<sup>1–5,21</sup> that the occurrence of the QHE is responsible for many of the characteristics of the anomalous region, the similarity between the proposed low-temperature–high-field state and the anomalous magnetotransport region in  $\alpha$ -(BEDT-TTF)<sub>2</sub>MHg(SCN)<sub>4</sub> ( $M = \text{K, Tl}$ ) gives rise to the conjecture that the QHE may be realized only within this state.

So far, there has been no comprehensive thermodynamic characterization of the low-temperature–high-field state, although Ref. 7 contained some thermodynamic evidence of the phase transition into this state. Its onset has mainly been associated with a decrease detected in the temperature dependence of the background interplane magnetoresistance.<sup>7,8,49</sup> Kartsovnik *et al.*<sup>7</sup> used the point of inflection and Sasaki *et al.*<sup>8</sup> the maximum seen in temperature sweeps to define the phase boundary. It is interesting to note that the observed fall in the background magnetoresistance at lower temperatures can be explained, at least partially, by the observed suppression of the maxima in the oscillatory part of the interplane magnetoresistance. As shown,<sup>3</sup>  $\rho_{zz}$  is mainly affected at fields at which the chemical potential resides between adjacent Landau levels, i.e., at integer  $F/B$ . The resistivity at values for which  $\mu$  lies within a Landau level appears to be much less affected.<sup>3,19</sup> Thus, with decreasing temperature, the resistivity at integer  $F/B$  is suppressed, and may eventually fall below the values at odd half-integer  $F/B$ . Consequently, the smoothly varying background resistance, as averaged over one wave form cycle, decreases as the temperature is lowered. Unless one chooses a value where  $F/B$  is exactly an odd half-integer, this effect will be ob-

served in temperature sweeps of the interplane magnetoresistance.

The reduction of the oscillation maxima, however, is only seen in interplane transport. de Haas–van Alphen oscillations, on the other hand, have been shown to exhibit conventional behavior at low temperatures<sup>3,4</sup> (also see Ref. 7). A definition of the phase boundary of the low-temperature–high-field state by association with the observed fall in the temperature dependence of  $\rho_{zz}$  is therefore ambiguous, as the decrease caused by the suppression of the oscillation maxima has to be taken into account. This decrease will be masking other effects which may be present. A very thorough study of the thermodynamic properties of the sample, e.g., the magnetization, is therefore necessary for the establishment of the exact phase boundaries and the true nature of the state.

## VII. CONCLUSION

In summary, we have carried out a comprehensive study of the high-field region of the organic conductors  $\alpha$ -(BEDT-TTF)<sub>2</sub>MHg(SCN)<sub>4</sub> ( $M = \text{K, Tl}$ ) over a wide range of angles, temperatures, and sweep rates. It is suggested that the “anomalous magnetotransport regime” is an intrinsic property of  $\alpha$ -(BEDT-TTF)<sub>2</sub>MHg(SCN)<sub>4</sub> ( $M = \text{K, Tl}$ ), and that its observation is only subject to sufficient sample quality. A detailed mapping of its occurrence has been carried out. The region of phase space occupied is found to be reminiscent of the recently proposed low-temperature–high-field state.

## ACKNOWLEDGMENTS

This work was supported by EPSRC and the Royal Society. The experimental work carried out at the Los Alamos National Laboratory was supported by the Department of Energy, the National Science Foundation and the State of Florida. The authors would like to thank Dieter Andres and Stephen Blundell for helpful discussions.

\*Present address: Department of Physics, Kyoto University, Kyoto 606-8502, Japan.

<sup>†</sup>Present address: Institut de Physique et Chimie des Matériaux de Strasbourg, 23 Rue du Loess, BP 20/CR, 67037 Strasbourg Cedex, France.

<sup>1</sup>N. Harrison, A. House, M.V. Kartsovnik, A.V. Polisski, J. Singleton, F. Herlach, W. Hayes, and N.D. Kushch, *Phys. Rev. Lett.* **77**, 1576 (1996); BEDT-TTF is bis(ethylenedithio)tetrathiafulvalene; for a review, see J. Singleton, *Rep. Prog. Phys.* **63**, 1111 (2000).

<sup>2</sup>N. Harrison, M.M. Honold, M.V. Kartsovnik, J. Singleton, S.T. Hannahs, D.G. Rickel, and N.D. Kushch, *Phys. Rev. B* **55**, R16 005 (1997).

<sup>3</sup>M.M. Honold, N. Harrison, J. Singleton, H. Yaguchi, C. Mielke, D. Rickel, I. Deckers, P.H.P. Reinders, F. Herlach, M. Kurmoo, and P. Day, *J. Phys.: Condens. Matter* **9**, L533 (1997).

<sup>4</sup>S. Hill, P.S. Sandhu, J.S. Qualls, J.S. Brooks, M. Tokumoto, N. Kinoshita, T. Kinoshita, and Y. Tanaka, *Phys. Rev. B* **55**, R4891 (1997).

<sup>5</sup>M.M. Honold, N. Harrison, J. Singleton, M.-S. Nam, S.J. Blundell, C.H. Mielke, M.V. Kartsovnik, and N.D. Kushch, *Phys. Rev. B* **59**, R10 417 (1999).

<sup>6</sup>For a review, see J. Singleton, *Phys. Mag.* **19**, 195 (1997).

<sup>7</sup>M.V. Kartsovnik, W. Biberacher, E. Steep, P. Christ, K. Andres, A.G.M. Jansen, and H. Müller, *Synth. Met.* **86**, 1933 (1997).

<sup>8</sup>T. Sasaki, A.G. Lebed, T. Fukase, and N. Toyota, *Phys. Rev. B* **54**, 12 969 (1996).

<sup>9</sup>M.M. Honold, N. Harrison, M.-S. Nam, J. Singleton, C.H. Mielke, M. Kurmoo, and P. Day, *Phys. Rev. B* **58**, 7560 (1998).

<sup>10</sup>R.H. McKenzie, G.J. Athas, J.S. Brooks, R.G. Clark, A.S. Dzurak, R. Newbury, R.P. Starrett, A. Skougarevsky, M. Tokumoto, N. Kinoshita, T. Kinoshita, and Y. Tanaka, *Phys. Rev. B* **54**, R8289 (1996).

<sup>11</sup>N. Harrison, E. Rzepniewski, J. Singleton, P.J. Gee, M.M. Honold, P. Day, and M. Kurmoo, *J. Phys.: Condens. Matter* **11**, 7229 (1999).

<sup>12</sup>N. Harrison, *Phys. Rev. Lett.* **83**, 1395 (1999).

<sup>13</sup>J.S. Brooks, G.J. Athas, S.J. Klepper, X. Chen, C.E. Campos, S. Valfells, Y. Tanaka, T. Kinoshita, M. Tokumoto, and H. Anzai, *Physica B* **201**, 449 (1994); J.S. Brooks, X. Chen, S.J. Klepper, S. Valfells, G.J. Athas, Y. Tanaka, T. Kinoshita, N. Kinoshita, M. Tokumoto, H. Anzai, and C.C. Agosta, *Phys. Rev. B* **52**, 14 457 (1995).

<sup>14</sup>T. Osada, R. Yagi, A. Kawasumi, N. Miura, M. Oshima, and G.

- Saito, Phys. Rev. B **41**, 5428 (1990).
- <sup>15</sup>T. Sasaki, H. Sato, and N. Toyota, Synth. Met. **41-43**, 2211 (1991).
- <sup>16</sup>M.V. Kartsovnik, D.V. Mashovets, D.V. Smirnov, V.N. Laukhin, A. Gilewski, and N.D. Kushch, J. Phys. I **4**, 159 (1994).
- <sup>17</sup>H. Mori, S. Tanaka, M. Oshima, G. Saito, T. Mori, Y. Maruyama, and H. Inokuchi, Bull. Chem. Soc. Jpn. **63**, 2183 (1990); D.-K. Seo, M.-H. Whangbo, B. Fravel, and L.K. Montgomery, Solid State Commun. **100**, 191 (1996).
- <sup>18</sup>A.A. House, S.J. Blundell, M.M. Honold, J. Singleton, J.A.A.J. Perenboom, W. Hayes, M. Kurmoo, and P. Day, J. Phys.: Condens. Matter **8**, 8829 (1996).
- <sup>19</sup>N. Harrison, R. Bogaerts, P.H.P. Reinders, J. Singleton, S.J. Blundell, and F. Herlach, Phys. Rev. B **54**, 9977 (1996).
- <sup>20</sup>*The Quantum Hall Effect*, edited by R.E. Prange and S.M. Girvin (Springer-Verlag, New York, 1990); T. Chakraborty and P. Pietenlaäinen, *The Quantum Hall Effects: Fractional and Integral* (Springer-Verlag, Berlin, 1995).
- <sup>21</sup>N. Harrison, J. Singleton, M.V. Kartsovnik, and F. Herlach, J. Phys.: Condens. Matter **9**, L47 (1997).
- <sup>22</sup>N. Dupuis and G. Montambaux, Phys. Rev. Lett. **68**, 357 (1992); Phys. Rev. B **46**, 9603 (1992).
- <sup>23</sup>A.E. Datars and J.E. Sipe, Phys. Rev. B **51**, 4312 (1995).
- <sup>24</sup>J.T. Chalker and A. Dohmen, Phys. Rev. Lett. **75**, 4496 (1995); J.T. Chalker and S.L. Sondhi, Phys. Rev. B **59**, 4999 (1999).
- <sup>25</sup>L. Balents and M.P.A. Fisher, Phys. Rev. Lett. **76**, 2782 (1996); S. Cho, L. Balents, and M.P.A. Fisher, Phys. Rev. B **56**, 15 814 (1997).
- <sup>26</sup>V.M. Yakovenko and H.-S. Goan, J. Phys. I **6**, 1917 (1996).
- <sup>27</sup>D.P. Druist, P.J. Turley, K.D. Maranowski, E.G. Gwinn, and A.C. Gossard, Phys. Rev. Lett. **80**, 365 (1998).
- <sup>28</sup>M. Kartsovnik (unpublished).
- <sup>29</sup>Interplane transport measurements of  $\alpha$ -(BEDT-TTF)<sub>2</sub>RbHg(SCN)<sub>4</sub> in pulsed magnetic fields can also be interpreted in this way [Fig. 1(b) of Ref. 10].
- <sup>30</sup>H. Yaguchi, N. Harrison, M.M. Honold, C. Mielke, J. Singleton, P.J. Gee, D. Rickel, I. Deckers, P.H.P. Reinders, F. Herlach, M. Kurmoo, and P. Day, Physica B **251**, 75 (1998).
- <sup>31</sup>L.I. Buravov, N.D. Kushch, V.N. Laukhin, A.G. Khomenko, E.B. Yagubskii, M.V. Kartsovnik, A.E. Kovalev, L.P. Rozenberg, R.P. Shibaeva, M.A. Tanatar, V.S. Yefanov, V.V. Dyakin, and V.A. Bondarenko, J. Phys. I **4**, 441 (1994).
- <sup>32</sup>In many highly anisotropic Q2D samples of irregular geometry and varying homogeneity, this is likely to represent the only way of obtaining a pure measurement of  $\rho_{||}$ . In contrast to  $\rho_{xy}$ ,  $\rho_{||}$  cannot be measured with great accuracy in steady-field experiments, as its even dependence on the field polarity prevents a removal of the residual  $\rho_{zz}$  component. With a knowledge of  $\rho_{xy}$  from steady-field measurements,  $\rho_{||}$  can subsequently be determined from the ratio of  $\rho_{xy}/\rho_{||}$ , contained in  $V_H$ .
- <sup>33</sup>The admixture of a Hall voltage component to the measured signal is expected whenever there is a radial distance between the voltage contacts (Ref. 5).
- <sup>34</sup>F. Herlach, Rep. Prog. Phys. **62**, 859 (1999).
- <sup>35</sup>J.E. Crow, D.M. Parkin, H.J. Schneider-Muntau, and N.S. Sullivan, Physica B **216**, 146 (1996).
- <sup>36</sup>N. Harrison, A. House, I. Deckers, J. Caulfield, J. Singleton, F. Herlach, W. Hayes, M. Kurmoo, and P. Day, Phys. Rev. B **52**, 5584 (1995).
- <sup>37</sup>J. Caulfield, S.J. Blundell, M.S.L. du Croo de Jongh, P.T.J. Hendriks, J. Singleton, M. Doporto, F.L. Pratt, A. House, J.A.A.J. Perenboom, W. Hayes, M. Kurmoo, and P. Day, Phys. Rev. B **51**, 8325 (1995).
- <sup>38</sup>P. Christ, W. Biberacher, H. Müller, K. Andres, E. Steep, and A.G.M. Jansen, Physica B **204**, 153 (1995).
- <sup>39</sup>T. Sasaki, W. Biberacher, and T. Fukase, Physica B **246-247**, 303 (1998).
- <sup>40</sup>The amplitude of the Shubnikov–de Haas oscillations has been renormalized through division by the smoothly varying background magnetoresistance [see *Magnetic Oscillations in Metals* (Ref. 41)].
- <sup>41</sup>D. Shoenberg, *Magnetic Oscillations in Metals* (Cambridge University Press, Cambridge, 1984).
- <sup>42</sup>J. Wosnitzer, *Fermi Surfaces of Low-Dimensional Organic Metals and Superconductors* (Springer-Verlag, Berlin, 1996).
- <sup>43</sup>S. Uji, J.S. Brooks, M. Chaparala, L. Seger, T. Szabo, M. Tokumoto, N. Kinoshita, T. Kinoshita, Y. Tanaka, and H. Anzai, Solid State Commun. **100**, 825 (1996).
- <sup>44</sup>T. Sasaki and T. Fukase, Phys. Rev. B **59**, 13 872 (1999).
- <sup>45</sup>For  $T < 1.2$  K and  $\theta > 30^\circ$ ,  $B_{inv}$  was obtained from extrapolations of the Fourier amplitude plots beyond the experimentally available field range. It was ensured that the fits were of sufficient accuracy.
- <sup>46</sup>G.J. Athas, S.J. Klepper, J.S. Brooks, M. Tokumoto, T. Kinoshita, N. Kinoshita, and H. Anzai, Synth. Met. **70**, 843 (1995).
- <sup>47</sup>*Proceedings of the International Conference on the Science and Technology of Synthetic Metals (ICSM)*, published biannually in Synth. Met.; see Synth. Met. **69-71** (1995); Synth. Met. **85-87** (1997); Synth. Met. **103** (1999).
- <sup>48</sup>N. Biskup, J.A.A.J. Perenboom, J.S. Brooks, and J.S. Qualls, Solid State Commun. **107**, 503 (1998).
- <sup>49</sup>S. Hill, J.S. Brooks, B.W. Fravel, L.K. Montgomery, M. Tokumoto, N. Kinoshita, T. Kinoshita, and Y. Tanaka, Synth. Met. **103**, 1807 (1999).
- <sup>50</sup>R. McKenzie, cond-mat/9706235 (unpublished); D. Zanchi, A. Bjeliš, and G. Montambaux, Phys. Rev. B **53**, 1240 (1996).
- <sup>51</sup>N.A. Fortune, M.A. Eblen, S. Uji, H. Aoki, J. Yamada, S. Tanaka, S. Maki, S. Nakatsuji, and H. Anzai, Synth. Met. **103**, 2078 (1999).
- <sup>52</sup>A.E. Kovalev, H. Müller, and M.V. Kartsovnik, Zh. Éksp. Teor. Fiz. **113**, 1058 (1998) [JETP **86**, 578 (1998)].
- <sup>53</sup>A.E. Kovalev, M.V. Kartsovnik, R.P. Shibaeva, L.P. Rozenberg, I.F. Schegolev, and N.D. Kushch, Solid State Commun. **89**, 575 (1994).
- <sup>54</sup>M.M. Honold, N. Harrison, C.H. Mielke, J. Singleton, M.C. Bennett, M. Kurmoo, and P. Day, Synth. Met. **103**, 2048 (1999).